Molecular Crystals and Liquid Crystals

Publication details, including instructions for authors and subscription information:
http://www.tandfonline.com/loi/gmcl20

Techniques to Characterize the Nonlinear Optical Response of Doped Nematic Liquid Crystals

V. Gayvoronsky [a], S. Yakunin [a], V. Nazarenko [a], V. Starkov [a] & M. Brodyn [a]

[a] Institute of Physics of NASU, Kyiv, Ukraine

Version of record first published: 31 Aug 2006

To cite this article: V. Gayvoronsky, S. Yakunin, V. Nazarenko, V. Starkov & M. Brodyn (2005): Techniques to Characterize the Nonlinear Optical Response of Doped Nematic Liquid Crystals, Molecular Crystals and Liquid Crystals, 426:1, 231-241

To link to this article: http://dx.doi.org/10.1080/15421400590891173

Mol. Cryst. Liq. Cryst., Vol. 426, pp. 231–241, 2005

ISSN: 1542-1406 print/1563-5287 online
DOI: 10.1080/15421400590891173

Taylor & Francis
Taylor & Francis Group

Techniques to Characterize the Nonlinear Optical Response of Doped Nematic Liquid Crystals

V. Gayvoronsky
S. Yakunin
V. Nazarenko
V. Starkov
M. Brodyn
Institute of Physics of NASU, Kyiv, Ukraine

We have examined the efficiency of various techniques for the determination of the nonlinear optical response (NLO) of dye-doped liquid crystals. The intensity ranges where each technique is optimal are defined. We propose an approach for precise and detailed NLO response measurements as a function of dye concentration when the optical parameters of samples vary in a wide range and change significantly after the light-induced Freedericksz transition.

Keywords: beam profile analysis; light-induced Freedericksz transition; liquid crystal; nonlinear optical response; organic dye

INTRODUCTION

The orientation of liquid crystal (LC) molecules and therefore the anisotropy of optical properties can be effectively driven by electrical and magnetic fields [1], as well as by intense optical irradiation [2,3]. The last phenomenon is called light-induced Freedericksz transition (LIFT) and has been extensively studied during last years [4]. The interest to the above phenomena came from the fact that the effective nonlinear optical (NLO) response of transparent LCs is 9 orders of magnitude larger than that for typical organic materials such as

This work was supported by the National Academy of Science of Ukraine, Grant # 1.4.1 B/109, and STCU, Grant #3091. We acknowledge to R. Vasyuta for the samples preparation.

Address correspondence to V. Gayvoronsky, Institute of Physics of NASU, Pr. Nauky 46, Kyiv, 03028, Ukraine. Tel.: 380-44-2650814, Fax: 380-44-265-15-89, E-mail: vlad@iop.kiev.ua

CS_2. A large enhancement of NLO properties was reported in [5] for LCs doped with a small amount of certain organic dyes. Depending on a specific dye utilized, the optical torque can be enhanced by one or two orders of magnitude.

Although the doping of LCs leads to a drastic decrease of the LIFT threshold, the realization of the effect requires significant laser intensities achieved with a focused continuous wave (CW) laser beam and reliable methods of detecting. LC is a material with multiple mechanisms that influence the NLO response; some of them have pronounced threshold character. A typical Z-scan technique is not suitable for the determination of NLO parameters below and above the LIFT threshold because it is impossible to obtain reversible Z-scan traces when the LIFT takes place in the laser waist region. The contribution of multiple NLO mechanisms and their cumulative effect prevent to properly separate and estimate the NLO responses with typical data processing algorithm [6]. For the different laser intensity ranges, the various NLO characterization techniques become more effective for a precise determination of the Freedericksz transition. For the complete investigation of NLO properties of a doped LC, we have used a set of various techniques and examined their efficiency in the intensity ranges below and above the LIFT. The proposed approach gives a possibility for the precise and detailed measurement of a NLO response of LC as a function of dye concentration when the optical parameters of samples vary in a wide range and change significantly after the LIFT threshold.

EXPERIMENTAL

In this work, the nematic LC material, 4′-n-pentyl-4-cyanobiphenyl (5CB), was used. The LC material was doped with the anthraquinone-containing (AQ) dye, *N,N′*-(4-methylphenyl)-1,4-diamino-AQ, of different concentrations (weight percentage from 0 up to 1.8, near the precipitation point). The molecule of this dye reveals an anisotropy of light absorption (i.e., it has a high magnitude of the dipole moment) and is perspective for the enhancement of the reorientation of nematic LC molecules. Experiments were performed for the cells with alignment induced by the coating of two glass substrates with a NiO cathode sputtered layer. The NiO layers provide a normal anchoring direction for 5CB molecules and, therefore, induce a homeotropic orientation in the whole cell. The thickness of the LC layer was set to be 10 micrometers.

The NLO experiments were carried out with a single-mode (TEM_{00}) CW He-Ne laser ($\lambda = 633$ nm, the power was 16 mW). The Gaussian spatial beam intensity profile distribution was controlled with a CCD array (AMKO LTI MuLTIray). NLO properties were characterized by investigating the distortion of a focused laser beam passing through the sample (the normal incidence condition) and variation of the sample transmittance as a function of the laser intensity (Fig. 1). The focal length of the lens was 11 cm. We positioned samples before and after the beam waist and varied the laser intensity with a neutral attenuator that does not deflect the beam. The experimental setup contains two photodiode channels. The first one (photodiode of this channel is indicated as P1 in Fig. 1) measures the laser beam power at the entrance of the optical system (the reference channel). The second channel (photodiode P2 or high dynamic range CCD-array) measures the power passed through the sample in different geometries:

1. Total transmitted power registration – the sample is positioned at the photodiode aperture to avoid energy losses due to the formation of ring pattern above the LIFT;

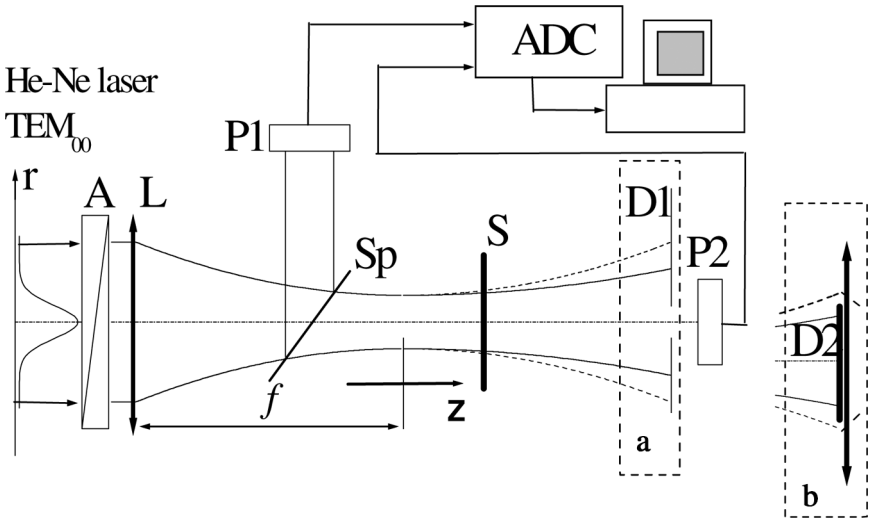

FIGURE 1 Experimental setup: **a)** optical scheme for measurements in the on-axis geometry, **b)** off-axis geometry. A – attenuator, Sp – beam splitters, D1 – diaphragm for on-axis measurements, D2 – for off-axis ones, L – focusing lens with focal length $f = 11$ cm, S – sample, P1 and P2 – photodiodes, ADC – analog-to-digital converter.

2. On-axis power registration in the far field – P2 collects on-axis part of the beam passed through finite aperture diaphragm D1 (Ø = 2 mm, the distance from the lens was 70 cm, Fig. 1a and Fig. 3);
3. Off-axis power registration in the far field – the on-axis region is blocked with opaque circle D2 mounted on the wide aperture collecting lens (the off-axis diaphragm, Fig. 1b and Fig. 3). The diameter of D2 is set to be larger (Ø = 6 mm) than the spot of the laser beam at intensities below the LIFT threshold.

RESULTS

1. The total transmittance as a function of the input laser intensity is presented in Figure 2. In these experiments, we positioned the wide-aperture photodiode P2 just after the cell in order to guarantee the separation of the photoinduced absorption from energy losses due to the influence of the NLO refractive index variation that results in a redistribution of the beam power and, therefore, the formation of aberrational rings after LIFT. The transmittance is about constant below the LIFT, and its small decrease for high AQ concentrations can be

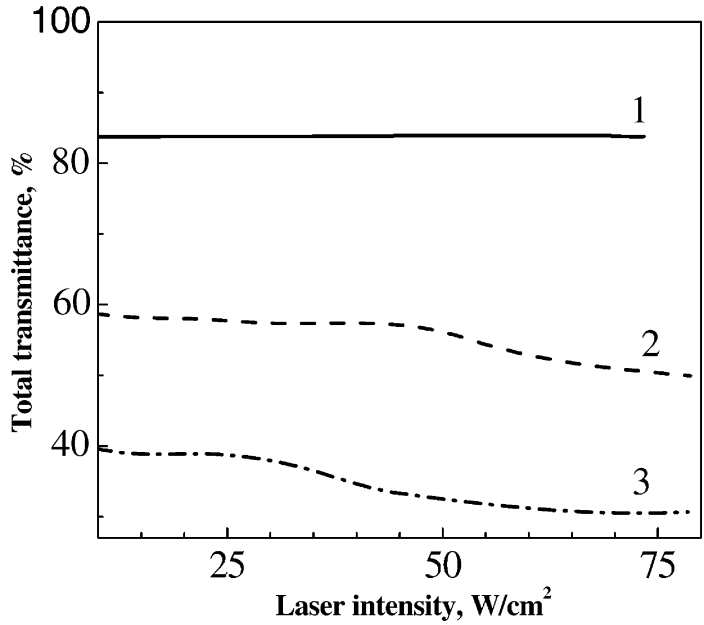

FIGURE 2 Total transmittance vs. laser intensity for different AQ dye concentrations: 1 – 0% (pure 5CB); 2 – 1%; 3 – 1.4%.

explained with the optical anisotropy of AQ dye molecules. Above the threshold, we observed up to a 10% of the photoinduced darkening of the cell caused by the reorientation of dye molecules. The extraordinary optical absorption coefficient corresponding to a planar alignment is higher than the ordinary absorption coefficient for a homeotropic LC alignment. The both values, the linear optical absorption and the photoinduced darkening increase with increase of the dye concentration. The smooth dependence of cell transmittance on the applied light intensity makes the total transmittance technique not applicable for the precise determination of the LIFT threshold.

2. The beam profiles passed through the LC cell are presented in Figure 3. The profiles were recorded in the far field region and normalized on input peak intensity. Just below the LIFT threshold, the beam profile (curve 2) keeps its shape close to a Gaussian one (curve 1), however the normalized intensity is higher in comparison with that in the low-intensity regime due to the self-focusing effect. The efficient narrowing of the beam gives an enhancement of the on-axis

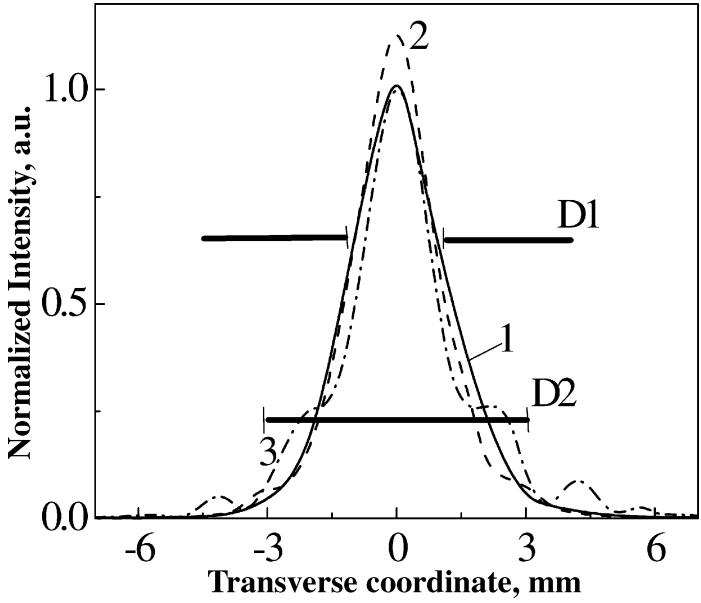

FIGURE 3 Transverse beam profiles at laser intensities: 1 – 0.3 W/cm^2, 2 – 22 W/cm^2, 3 – 25 W/cm^2. The 5CB + 1.4% AQ dye cell is positioned 3 cm after the beam waist, the registration is carried out at 70 cm after the lens. Each profile is normalized on the input peak laser intensity.

transmittance through diaphragm D1. After the LIFT, the reorientation of LC molecules causes the extremely large NLO variation of the refractive index. In the far field one can observe formation of aberrational rings (curve 3) caused by the inhomogeneous NLO phase modulation across the beam in the cell. The radius of dark rings and their number increase with the laser intensity. Such energy redistribution between the central and peripheral parts of the beam leads to a decrease of the on-axis transmittance and may be attributed to a self-defocusing effect. Our simulations of experimental data demonstrate that the variation of refractive index as function of intensity remains positive after the LIFT.

The on-axis transmittance in the far field, when the beam passes through the finite aperture diaphragm is rather sensitive to the convergence or divergence of the beam due to the effective photoinduced LC refractive index response. The size of the diaphragm D1 is less than the beam diameter in the low-intensity limit. For pure 5CB, we observed the increase of the on-axis transmittance (Fig .4) when the sample was positioned after the beam waist (solid lines in Fig. 4)

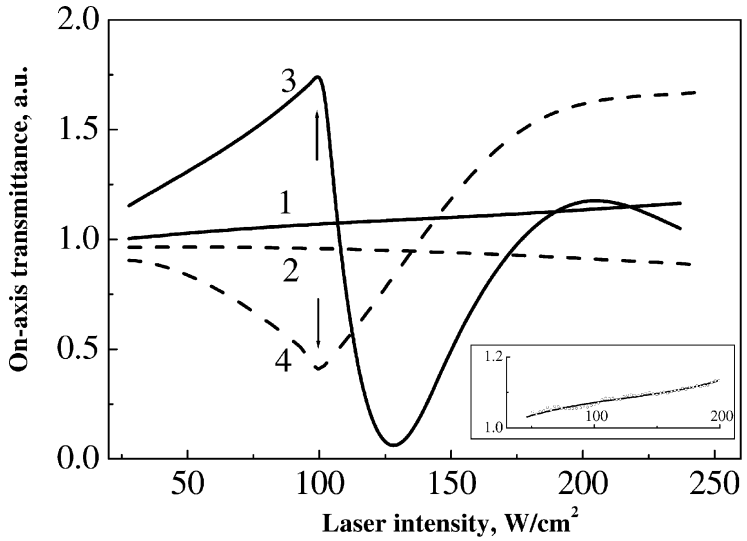

FIGURE 4 Normalized on-axis transmittance vs. laser intensity for different LC positions towards the beam waist: solid lines –1cm after the waist, dashed –1cm before the waist. Curves 1, 2 – pure 5CB; 3, 4 – 5CB + 0.4% AQ dye. Arrows mark the LIFT threshold. Insert - experimental data (dots) and simulation result (solid line) according model (2) for the pure 5CB cell (curve 1).

and this transmittance was decreased when the sample was positioned at the same distance before the waist (dashed lines in Fig. 4). Such a behavior is generally attributed to the self-focusing effect (the positive refractive index variation with light intensity) [7]. For the sample doped with AQ dye (Fig. 4 curves 3, 4), we observed larger slopes on the on-axis transmittance curves. The slope magnitude is proportional to the on-axis NLO phase shift $\varphi_{nl} = kLn_2I_0$ and can be used for the calculation of the cubic NLO response. Here k is the wavenumber, I_0 is the on-axis laser intensity, n_2 is the NLO refractive index coefficient defined from NLO index variation $\Delta n = n_2I_0$, L is a cell thickness.

A small variation of the photoinduced absorption gives the possibility to apply the thin NLO lens model approach and the Gaussian decomposition technique to the description of a transmitted laser beam in the far field. The model describes the propagation of a laser beam through the sample with cubic NLO response. The NLO phase modulation due to the self-action effect transforms the initial Gaussian laser beam (TEM_{00} mode) into the infinite set of Gaussian beams with different radii and wavefront curvatures. The amplitude of each beam is proportional to corresponding power of φ_{nl},

$$E_a(r) = E_0 \exp\left(\frac{-\alpha L}{2}\right) \sum_m^{\infty} \frac{[i\varphi_{nl}]^m}{m!} \cdot \frac{w_{m0}}{w_m} \cdot \exp\left(-\frac{r^2}{w_m^2} - \frac{ikr^2}{2R_m} + i\theta_m\right), \quad (1)$$

where E_0 is the incident laser field at the sample, r is the transverse coordinate, d is the distance from the sample to the registration plane P2, w is the radius and R is the wavefront curvature of the laser beam at the plane of the sample; α is the linear absorption coefficient, w_{m0}, w_m, R_m, and θ_m are the geometry-defined parameters [6]:

$$w_{m0}^2 = w^2/(2m+1), \qquad w_m^2 = w_{m0}^2\left[g^2 + (d/d_m)^2\right],$$
$$d_m = kw_{m0}^2/2, \qquad R_m = d\left[1 - g/(g^2 + (d/d_m)^2)\right],$$
$$\theta_m = \tan^{-1}[d/(d_m \cdot g)], \qquad g = 1 + d/R$$

The on-axis transmittance is obtained by integration of the module square, Eq. 1, of the laser field over the diaphragm aperture and than normalized by the total beam power. The analytical expression for the on-axis transmittance is

$$T_a(I_0) = S \cdot \left[1 + a_1 \cdot \varphi_{nl} + a_2 \cdot (\varphi_{nl})^2 + a_3 \cdot (\varphi_{nl})^3 + \cdots\right], \quad (2)$$

where S and a_i are coefficients defined by the geometry of the experiment:

$$S = 1 - \exp\left\{-2(r_0 k w)^2 / \left[4z^2(1+\beta^2)\right]\right\}$$

$$a_1 = \frac{1}{S}\exp\left(-\frac{4r_0^2(3+b^2)}{w^2(9+b^2)}\right)\sin\left(\frac{8r_0^2 b}{w^2(9+b^2)}\right)$$

$$a_2 = \frac{1}{3S}\left[\exp\left(-\frac{6r_0^2(5+b^2)}{w^2(25+b^2)}\right)\times\cos\left(\frac{24br_0^2}{w^2(25+b^2)}\right) - \exp\left(-\frac{6r_0^2(1+b^2)}{w^2(9+b^2)}\right)\right].$$

Here, r_0 is the radius of aperture D1, $b = -(1-z/R)\left(2z/kw^2\right)^{-1}$ is the ratio of the geometric divergence (the resulting action of the optical system) and the diffraction divergence of the laser beam.

The averaged on-axis transmittance intensity dependences are shown in Figure 4 (maximum deviation from the experimental points is less than 1%). To obtain sign and magnitude of the NLO response we fitted the experimental data using expansion of φ_{nl} represented by Eq. 2. The experimental points and simulation curve for the pure 5CB cell are demonstrated in Figure 4, see insert. The NLO refractive coefficient n_2 sharply increases with the dye concentration (Table 1). Positive slope of the transmittance as a function of the laser intensity (curves 1 and 3 – the cells are positioned after the beam waist) and the negative one (curves 2 and 4 – the cells are positioned at the same distance before the waist) correspond to the self-focusing effect. The magnitudes of the transmittance variation are almost equal for positive and negative slope, that gives the same value of the coefficient n_2 for both samples positions.

The on-axis transmittance technique is precise enough to estimate cubic NLO susceptibility within the range below the LIFT, since the single-mechanism of NLO response is applied in the model. This technique is also applicable to the determination of the LIFT threshold. However for the samples with a high AQ concentration the

TABLE 1 The Light-induced Freedericksz Transition (LIFT) Threshold for Different Dye Concentrations and Estimated Values of the Cubic NLO n_2 Coefficient and $\chi^{(3)}$ Below and Above the LIFT

AQ dye, %	Cubic nonlinearity below the LIFT		LIFT threshold, W/cm^2	Cubic nonlinearity above the LIFT	
	n_2, cm^2/MW	$\chi^{(3)}$, esu		n_2, cm^2/MW	$\chi^{(3)}$, esu
0	8.2	4.5×10^{-4}	2650	–	–
1.4	515	2.84×10^{-2}	20	1.0×10^{4}	5.5×10^{-1}

photoinduced darkening of the samples suppresses the transmittance, therefore the sharpness of the LIFT decreases that may result in a mistake for the LIFT threshold.

3. In order to precisely determine the LIFT threshold, we applied off-axis transmittance measurements. We located the opaque circle diaphragm D2 (Fig. 1b) just behind the wide aperture focusing lens. The diaphragm blocked the central area the beam, so that the lens converged the only peripheral part of a beam. Before the LIFT, the variation of the photoinduced refractive index does not significantly influence the beam profile. Resulting signal on P2 photodiode is zero. After the LIFT threshold, the energy redistribution across the beam leads to the formation of aberrational rings and therefore to sharp increase of the off-axis transmittance, see Figure 5. Since the off-axis transmittance arises practically from zero point, the signal-to-noise ratio in this geometry is extremely high. This technique is most acceptable for determination of the LIFT threshold especially for samples doped with high concentration of dyes.

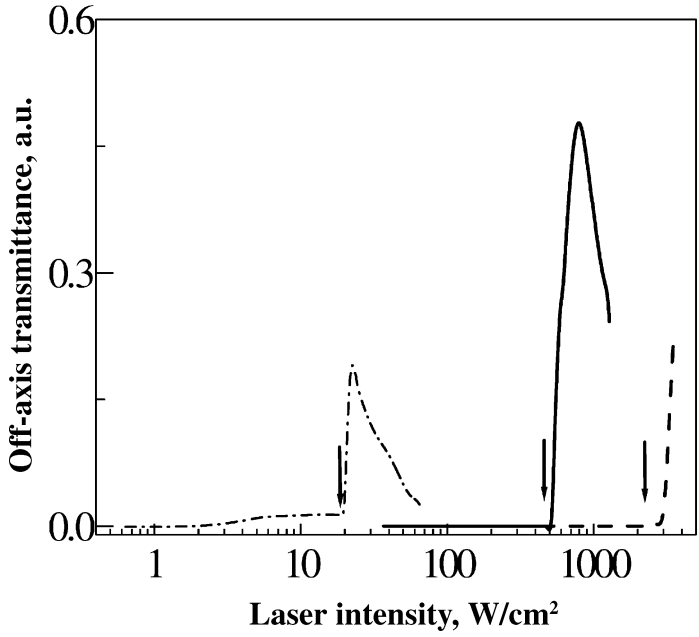

FIGURE 5 Off-axis transmittance versus laser intensity for different AQ dye concentrations: 1 - - - 0% (pure 5CB); 2 —— 1%; 3 –·–· 1.4%. Arrows mark the LIFT threshold.

To estimate the NLO response after the LIFT threshold, we performed analysis of the beam profile distortion in the far field. In comparison with the on-axis transmittance approach, where we studied the dependences of sample transmittance as a function of the laser intensity, the analyses of the intensity redistribution across a beam in the far field was performed for defined laser intensity. Within this approach, we performed the least squares fitting of the experimentally obtained profile (circles in Fig. 6) with the theoretical model (the line in Fig. 6) of photoinduced NLO lens for a given laser intensity. Due to the extremely effective NLO phase shift ($\varphi_{nl} \sim 5.4\pi$, the estimation accuracy is about 5%), we take into account more than 400 terms in expansion (1). The shift φ_{nl} corresponds to the positive cubic NLO refractive index coefficient $n_2 = (1 \pm 0.15) \times 10^4\,\mathrm{cm}^2/\mathrm{MW}$ ($\chi^{(3)} = 5.5 \times 10^{-1}$ esu). The resulted value is 50% less, $n_2 = 2.1 \times 10^4\,\mathrm{cm}^2/\mathrm{MW}$, than that obtained within the geometric optics approach [3], where φ_{nl} is taken from the number of dark rings in the beam cross-section. We explain the difference in experimental and theoretical curves at $r = 1.4\,\mathrm{mm}$, where theory predicts the zero intensity, due to the fact that the CCD-array has finite vertical size

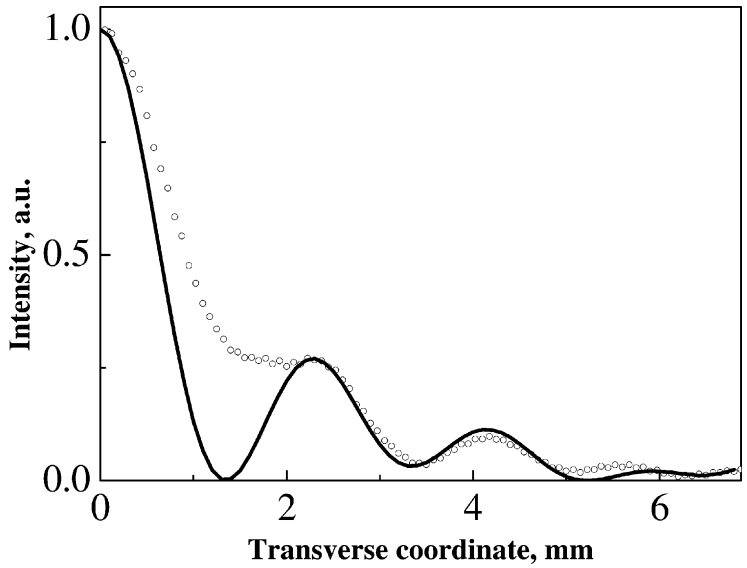

FIGURE 6 Comparison of the recorded beam profile in the far field (dots) with simulation data (solid line) for the 5CB + 1.4% AQ dye cell and an input peak laser intensity of $25\,\mathrm{W/cm}^2$. The cell position is 3 cm after the beam waist, the registration is made at the distance of 70 cm after the lens.

of its elements, which causes the blurring of the exact minima condition. The magnitude of the NLO response after the LIFT is more than one order of magnitude larger in comparison with the corresponding value before the LIFT threshold, $n_2 = 515\,\mathrm{cm}^2/\mathrm{MW}$ (see Table 1).

CONCLUSIONS

NLO properties of a dye doped LC have been investigated using different techniques: total transmitted power registration; on-axis power registration in the far field; off-axis power registration in the far field. We have examined their efficiency in the intensity ranges below and above the LIFT. The NLO response of the dye-doped LC reveals a large difference (by one order of magnitude) for cubic susceptibilities measured below and above the light-induced Freedericksz transition. The intensity variation of the on-axis transmittance is the most precise technique for the NLO response characterization within the range of a monotonic behavior of transmittance that is observed below the LIFT. After the LIFT, the analysis of beam profile (off-axis power registration) is more applicable. The on-axis and off-axis transmittance techniques are applicable for the LIFT threshold determination; the last one is the most effective for the samples with a high AQ concentration.

REFERENCES

[1] de Gennes, P. G. & Prost, J. (1993). *The physics of liquid crystals*, Oxford University Press: Oxford.
[2] Ya. Zel'dovich, B., Pilipetskii, N. F., Sukhov, A. V., & Tabiryan, N. V. (1980). *Sov. Phys. JETF Lett.*, *31*, 263.
[3] Zolot'ko, A. S., Kitaeva, V. F., Sobolev, N. I., & Suhorukov, A. S. (1981) *Sov. Phys. JETF*, *81*, 933.
[4] Marrucci, L. (2002). *Liquid Crystal Today, 11*(3), 1.
[5] Janossy, I. & Kosa, T. (1992) *Opt. Lett.*, *17*, 1183.
[6] Sheik-Bahae, M., Said, A., Wei, T.-H., Hagan, D., & Van Stryland, E. W. (1990). *J. Quant Elect.*, *4*, 760.
[7] Brodyn, M. S., Borshch, A. A., & Volkov, V. I. (1990). *Refractive nonlinearity of wide-gap semiconductors and applications*, Harwood Academic Publishers: London.